Am. J. Hum. Genet. 73:835–848, 2003

Confirmation of the Type 2 Myotonic Dystrophy $(CCTG)_n$ Expansion Mutation in Patients with Proximal Myotonic Myopathy/Proximal Myotonic Dystrophy of Different European Origins: A Single Shared Haplotype Indicates an Ancestral Founder Effect

Linda L. Bachinski,[1] Bjarne Udd,[2,3] Giovanni Meola,[4] Valeria Sansone,[4] Guillaume Bassez,[5] Bruno Eymard,[6] Charles A. Thornton,[7] Richard T. Moxley,[7] Peter S. Harper,[8] Mark T. Rogers,[8] Karin Jurkat-Rott,[9] Frank Lehmann-Horn,[9] Thomas Wieser,[10] Josep Gamez,[11] Carmen Navarro,[12] Armand Bottani,[13] Andre Kohler,[14] Mark D. Shriver,[15] Riitta Sallinen,[16,18] Maija Wessman,[16,18] Shanxiang Zhang,[19] Fred A. Wright,[20] and Ralf Krahe[1,17,19]

[1]Section of Cancer Genetics, Department of Molecular Genetics, University of Texas M. D. Anderson Cancer Center, Houston; [2]Department of Neurology, Vaasa Central Hospital, Vaasa, Finland; [3]Department of Neurology, Tampere University Hospital, Tampere, Finland; [4]Department of Neurology, San Donato Hospital, Milan; [5]Department of Pathology, Henri Mondor University Hospital, Créteil, France; [6]Myology Institute, Salpêtrière Hospital, Paris; [7]Department of Neurology, University of Rochester Medical Center, Rochester, NY; [8]Institute of Medical Genetics, University Hospital of Wales, Cardiff; [9]Department of Applied Physiology, University of Ulm, Ulm, Germany; [10]Department of Neurology, University of Halle, Halle, Germany; [11]Department of Neurology, General Hospital Vall d'Hebron University, Barcelona; [12]Department of Anatomical Pathology, Meixoeiro Hospital, Vigo, Spain; [13]Division of Medical Genetics and [14]Department of Neurology, Geneva University Hospitals, Geneva, Switzerland; [15]Department of Anthropology, Pennsylvania State University, University Park; [16]Department of Clinical Chemistry and [17]Folkhälsan Institute of Genetics, University of Helsinki, and [18]Research Program of Molecular Medicine, Biomedicum Helsinki, Helsinki; [19]Human Cancer Genetics Program, Department of Molecular Virology, Immunology and Medical Genetics, Comprehensive Cancer Center, Ohio State University, Columbus; and [20]Department of Biostatistics, University of North Carolina, Chapel Hill

Myotonic dystrophy (DM), the most common form of muscular dystrophy in adults, is a clinically and genetically heterogeneous neuromuscular disorder. DM is characterized by autosomal dominant inheritance, muscular dystrophy, myotonia, and multisystem involvement. Type 1 DM (DM1) is caused by a $(CTG)_n$ expansion in the 3′ untranslated region of *DMPK* in 19q13.3. Multiple families, predominantly of German descent and with clinically variable presentation that included proximal myotonic myopathy (PROMM) and type 2 DM (DM2) but without the DM1 mutation, showed linkage to the 3q21 region and were recently shown to segregate a $(CCTG)_n$ expansion mutation in intron 1 of *ZNF9*. Here, we present linkage to 3q21 and mutational confirmation in 17 kindreds of European origin with PROMM and proximal myotonic dystrophy, from geographically distinct populations. All patients have the DM2 $(CCTG)_n$ expansion. To study the evolution of this mutation, we constructed a comprehensive physical map of the DM2 region around *ZNF9*. High-resolution haplotype analysis of disease chromosomes with five microsatellite and 22 single-nucleotide polymorphism markers around the DM2 mutation identified extensive linkage disequilibrium and a single shared haplotype of at least 132 kb among patients from the different populations. With the exception of the $(CCTG)_n$ expansion, the available markers indicate that the DM2 haplotype is identical to the most common haplotype in normal individuals. This situation is reminiscent of that seen in DM1. Taken together, these data suggest a single founding mutation in DM2 patients of European origin. We estimate the age of the founding haplotype and of the DM2 (CCTG) expansion mutation to be ~200–540 generations.

Introduction

Myotonic dystrophy (DM) is the most common muscular dystrophy in adults, with an incidence for type 1 DM (DM1 [MIM 160900]) of ~1/8,000 individuals in western European and North American populations (Harper 2001). DM is a clinically and genetically heterogeneous neuromuscular disorder characterized by autosomal dominant inheritance, muscular dystrophy, myotonia, and multisystem involvement (International Myotonic Dystrophy Consortium 2000; Harper 2001; Mankodi and Thornton 2002). DM1 is caused by a $(CTG)_n$ expansion in the 3′ UTR of the DM protein kinase gene (*DMPK*) in 19q13.3. Clinically distinct forms not associated with the DM1 $(CTG)_n$ expansion and unlinked to 19q13.3 have been described (Abbruzzese et al. 1996), including proximal myotonic myopathy (PROMM [MIM 600109]) (Ricker et al. 1994, 1995; Thornton et al. 1994; Meola

Received May 8, 2003; accepted for publication July 18, 2003; electronically published September 10, 2003.

Address for correspondence and reprints: Dr. Ralf Krahe, Section of Cancer Genetics, Unit 11, Department of Molecular Genetics, Room Y7.6032, University of Texas M. D. Anderson Cancer Center, 1515 Holcombe Blvd., Houston, TX 77030-4009. E-mail: RalfKrahe@mdanderson.org

0002-9297/2003/7304-0012$15.00

et al. 1996; Phillips et al. 1998; Newman et al. 1999; Kohler et al. 2000; Kress et al. 2000; Wieser et al. 2000; Bassez et al. 2001), proximal myotonic dystrophy (PDM) (Udd et al. 1997), and type 2 DM (DM2 [MIM 602668]) (Day et al. 1999), which are characterized by either predominantly proximal (PROMM and PDM) or distal and proximal (DM2) muscle involvement (Moxley et al. 1998). The mutation underlying DM2 and a subset of PROMM was mapped to 3q21.3 (Ranum et al. 1998; Ricker et al. 1999) and was recently identified as an unstable $(CCTG)_n$ expansion in intron 1 of *ZNF9* (Liquori et al. 2001). Affected families were predominantly of German or Polish origin (Day et al. 2003).

Similar to DM1 (Ashizawa and Epstein 1991), DM2 and PROMM appear to be more prevalent in populations of European descent and, to date, have not been reported in other populations (Moxley et al. 2002). In DM1, there is striking linkage disequilibrium (LD) around the $(CTG)_n$ expansion (Imbert et al. 1993; Neville et al. 1994; Yamagata et al. 1996). With the exception of one sub-Saharan kindred (Krahe et al. 1995), a single haplotype within and flanking *DMPK* has been shown to be in complete LD with DM1. This has been interpreted as indicating that either predisposition for $(CTG)_n$ instability resulted from a founder effect, which occurred only once or a few times in human evolution, or elements within the disease haplotype predispose the $(CTG)_n$ repeat to instability (Mahadevan et al. 1993; Neville et al. 1994).

The phenotypic similarities between patients with DM2 and PROMM, who have linkage to 3q21 and the DM2 $(CCTG)_n$ expansion, and patients with other related myotonic myopathies raised the possibility of a similar mutation in kindreds initially classified as affected with a clinically distinct phenotype (Moxley et al. 1998). Moreover, we reasoned that kindreds with DM2 representing a greater breadth of geographic origin would be needed to rule out linkage heterogeneity and to provide greater detail on a possible ancestral haplotype. Here, we present evidence of linkage to 3q21 and mutational verification of the DM2 $(CCTG)_n$ expansion in 17 kindreds with PROMM and PDM from geographically separate populations of European origin. High-resolution haplotype analysis of disease chromosomes around the $(CCTG)_n$ expansion identified extensive LD and a single shared disease haplotype in patients with DM2 of European descent, suggesting a founder effect similar to that seen for the $(CTG)_n$ expansion mutation in DM1.

Subjects and Methods

Subjects and Kindreds

Enrollment of participants for this study was approved by the respective institutional review boards. Participants were recruited by their attending physicians. After obtaining informed consent, blood was drawn and DNA prepared using GenePure (Gentra). For clinical diagnosis, the criteria of the International Working Group on PROMM and Other Proximal Myotonic Syndromes were used (Moxley et al. 1998). Deceased family members were considered affected on the basis of history. We ascertained 17 unrelated pedigrees from Germany (4), Finland (3), Italy (3), the United States (2), France (2), Spain (1), Switzerland (1) and the United Kingdom (1) with similar clinical phenotypes, some of which were previously described (Meola et al. 1996; Udd et al. 1997; Phillips et al. 1998; Kohler et al. 2000; Kress et al. 2000; Wieser et al. 2000; Bassez et al. 2001). The DM1 $(CTG)_n$ triplet expansion was ruled out in all patients (Brook et al. 1992).

Linkage Analysis

Linkage analysis was performed using FASTLINK (Schaffer 1996), GENEHUNTER (Kruglyak et al. 1996), and SIMPLE (Irwin et al. 1994). Age-dependent penetrance classes were designated for at-risk unaffected individuals on the basis of the combined age-at-onset profile for the respective kindreds. A phenocopy rate of 0.0002 was based on the incidence of myotonic discharges in the general population (1/5,000).

Genetic and Physical Map of the DM2 Region

Initially, 27 microsatellite markers (23 from the Marshfield map and 4 novel markers derived from BAC sequences) flanking the DM2 locus and spanning ~11 Mb (10.5 cM on the sex-averaged map) were genotyped in families with DM2 (fig. 1*A*). Novel markers are described in table A (online only).

BAC clones containing sequences from the *ZNF9* region were identified using the UCSC Genome Browser (April 2002, June 2002, and November 2002 builds). *ZNF9* is on BACs RP11-814L21 (GenBank accession number AC022944) and RP11-309B5 (GenBank accession number AC135587). On the centromeric side, 814L21 overlaps RP11-723O4 (GenBank accession number AC112484) and RP11-434H6 (GenBank accession number AC108673). On the telomeric side, there is a gap of indeterminate size before the next contig (GenBank accession number NT_006025). The approximate size of the gap between 814L21 and RPC1-3_436B3 was determined by fiber-FISH (see below). The BAC contig map is shown in figure 1*B*.

Using the Sequencher program (GeneCodes), we assembled the sequences of the four BACs with each other and divided 814L21 into four bins on the basis of overlap (fig. 5). Additional pieces of 309B5 totaling ~30 kb do not overlap the other clones and are assumed to be telomeric to *ZNF9*. As of the November 2002 build, exact sizes can be calculated for bins I–III. The estimated

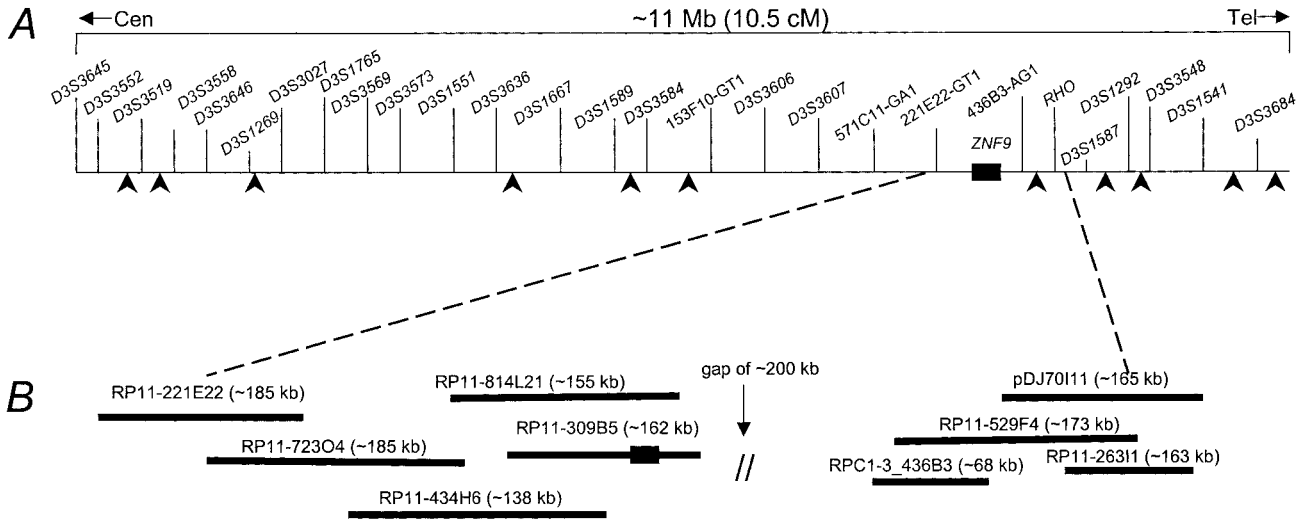

Figure 1 Physical and genetic map of the DM2 region in 3q21. *A*, Locations of the 27 microsatellite markers used. Marker order was determined initially through use of the deCODE map (Kong et al. 2002) and then was refined using physical locations and by minimizing recombinations in the families tested. Locations of recombinations observed are indicated by arrowheads. *B*, BAC clones used to map markers close to *ZNF9*.

size for 309B5 was based on unfinished sequence. Because some of the published sequence of 814L21 appears to be derived from chromosome 5, we estimated the size of 814L21 as the minimum size determined by overlap with the other BACs. All five exons of *ZNF9* are found within bin IV on two contigs totaling 19.8 kb, with *ZNF9* occupying a minimum of 13 kb. Exons 1 and 2 of *ZNF9* are separated by a large intron that is reported to be >20 kb (Liquori et al. 2001), although only 11.7 kb could be accounted for in this assembly. The remaining sequence in bin IV must be located either within this large intron or telomeric to the gene. Figure 5 shows the remaining four contigs of bin IV as being located within intron 1, resulting in a maximum size for *ZNF9* of 44 kb.

Physical Mapping of Genomic Clones by FISH

Metaphase FISH was used to verify that 814L21 was not chimeric, and fiber-FISH was used to estimate the size of the gap telomeric to *ZNF9* (fig. 3). Metaphase chromosomes and extended DNA fibers were prepared from peripheral blood lymphocytes of a healthy individual (Heiskanen et al. 1994; Sallinen et al. 2001). BACs 814L21 and 529F4 and PAC 436B3 were used as hybridization probes (fig. 3*C*). The clones were obtained from the BACPAC Resource Center (Children's Hospital Oakland Research Institute) and were grown by standard methods; DNA was extracted using the Qiagen Large Construct Kit. Probes for FISH were labeled with either biotin-16-dUTP or digoxigenin-11-dUTP (Roche Diagnostics), by nick translation using standard protocols. FISH and the analysis of hybridization signals were performed as described elsewhere (Sallinen et al. 2001).

Identification of Microsatellite Markers near ZNF9

We interrogated the sequence of 814L21 for microsatellite repeat sequences. In addition to the $(GT)_n$ repeat that is directly adjacent to the DM2 $(CCTG)_n$ expansion in *ZNF9*, we identified two microsatellites, 814L21-GT1 (CL3N59 [Liquori et al. 2001]) and 814L21-GT2 (fig. 5). Proximal to *ZNF9* on 221E20, we identified a $(GT)_n$ repeat, 221E20-GT1 (CL3N99 [Liquori et al. (2001]). Distal to *ZNF9*, on 436B3, we identified a complex $(AG)_n/(CT)_n$ repeat (436B3-AG1). All novel markers were confirmed by STS-content mapping of the respective BAC DNAs. Forward primers were tagged fluorescently (FAM or HEX), and reverse primers had 5′ tails (5′-GTTTCTT-3′), to facilitate nontemplated polyadenylation of the PCR product (Brownstein et al. 1996). Primer sequences for all novel microsatellite markers are described in table A (online only).

Identification of SNPs near ZNF9

To saturate the *ZNF9* region with markers, we interrogated various databases (CGAP Gene Viewer Web site; dbSNP Home Page; NCBI Reference Sequence (RefSeq) Web site; The SNP Consortium Web site) for SNPs in the *ZNF9* region. Two coding SNPs were identified, neither of which alters an amino acid: CGAP_866183 (Gly36Gly) in exon 2 and CGAP_866189 (Asp52Asp) in exon 3. Intragenic noncoding SNP CGAP_866187 is in exon 2 in the 5′ UTR, and CGAP_866192 and

CGAP_866191 are in exon 5 in the 3′ UTR. These five SNPs are all within 2.5 kb of the DM2 repeat. TSC873597 and TSC548022 are immediately adjacent to exon 1, and TSC1065149 is just centromeric to *ZNF9*. We selected additional SNPs that were predicted to be within or immediately adjacent to *ZNF9*. In all, we interrogated 22 SNPs, all of which were verified to be on 814L21 by STS-content mapping and were present in our assembly on multiple BACs. Locations of all markers are shown in figure 5.

Genotyping of Microsatellites and SNPs

Amplification of microsatellites was performed on an ABI 9700 thermocycler, using the Qiagen Hot Start Master Mix. Amplification products were pooled as appropriate and were analyzed by capillary electrophoresis on an ABI 3100 Genetic Analyzer. Amplification from BACs was as above, using 2 ng of template DNA.

Most SNPs were genotyped by sequencing; all sequencing primers were synthesized with M13 tails (table B [online only]). Amplification was as for microsatellites; products were cleaned using a Qiagen 96-well vacuum manifold. Sequencing reactions were performed using BigDye Terminator version 3.0 chemistry under standard conditions, and products were purified by ethanol precipitation, dehydrated in a vacuum centrifuge, and resuspended in 20 μl formamide before capillary electrophoresis on an ABI 3100 Genetic Analyzer.

Five *ZNF9* intragenic SNPs were typed by pyrosequencing. A biotinylated universal primer was used in the amplification, and a universal tail was used on the appropriate primer to generate biotinylated products for pyrosequencing (table C [online only]) (Colella et al. 2003), which was conducted according to manufacturer's directions. For the intragenic SNP TSC873597, the polymorphism alters a *Hae*III restriction site and was genotyped by *Hae*III (Promega) digestion according to the manufacturer's suggestions and visualized on 4% Metaphor (FMC) gels.

Genotyping of Normal and Mutant $(CCTG)_n$ Alleles in ZNF9

Normal alleles were detected by PCR across the DM2 repeat (Liquori et al. 2001). To confirm whether individuals showing a single allele had a second expanded allele resistant to PCR, we designed a repeat-primed PCR (RP-PCR) assay analogous to similar assays for DM1 (Warner et al. 1996; Sermon et al. 2001) and SCA10 (Matsuura and Ashizawa 2002). Primer sequences are shown in table D (online only). Each 15-μl amplification reaction contained 14 ng genomic DNA, 200 pmol of DM2-RP-F, 20 pmol of DM2-RP-R4, and 180 pmol of the universal primer. Qiagen Hot Start Mix was used according to the manufacturer's directions. Cycling conditions consisted of initial denaturing at 95°C for 15 min; 35 cycles of 95°C for 45 s, 60°C for 45 s, and 72°C for 2 min; followed by a final extension step at 72°C for 7 min. Products were subjected to capillary electrophoresis on an ABI 3100 Genetic Analyzer, and results were viewed using the Genotyper program.

DM2 $(CCTG)_n$ Expansion Detection by Field Inversion Electrophoresis (FIGE)

For Southern blot detection of the DM2 $(CCTG)_n$ expansion, 5–10 μg of high-molecular-weight genomic DNA extracted from peripheral blood leukocytes or lymphoblastoid cell lines by standard techniques were digested with *Eco*RI (NEB). For each kindred, one parent-offspring pair (when available) and one unaffected founder or pedigree member were examined. To obtain adequate resolution in the range of expansion, FIGE was used. In brief, digested samples were separated by electrophoresis on 1% agarose (BIO-RAD) on the FIGE Mapper (BIO-RAD), using program 3 (180 V forward, 120 V reverse, and switch time ramp 0.12.0 s, linear shape) for 13 h. Samples were transferred to Hybond N^+ blotting membranes (Amersham). Detection was with a probe specific for the DM2 $(CCTG)_n$ expansion (Liquori et al. 2001) in RapidHyb solution (Amersham), using standard serial stringency washes followed by phosphorimaging and/or autoradiography.

Selection and Preparation of Samples

To determine whether a unique haplotype segregates with the DM2 expansion, we selected families in which the DM2 expansion was segregating and families with normal alleles. In all, 265 individuals were studied. From the families with DM2, we chose 60 affected and 38 normal individuals, as well as 30 index cases. Control families were selected from the same ethnic backgrounds as the families with DM2 and included 126 members of 13 families and 11 unrelated individuals. Four monoallelic somatic cell hybrid lines resulting from diploid-to-haploid conversion (Yan et al. 2000), each containing one chromosome 3 homologue from a Finnish patient with DM2 (two normal and two DM2 lines), served as controls. A 16-sample screening panel included the four hybrid lines. Markers that showed at least one heterozygous individual in the screening set were genotyped on all samples.

Analysis of Data

Population allele frequencies for all markers were calculated using independent normal chromosomes, both phase-known and phase-unknown. For haplotype analysis, only phase-known independent DM2 and normal chromosomes were used. Multipoint linkage analysis and haplotype construction were conducted with GENE-

HUNTER. In all, we were able to unequivocally characterize 17 independent phase-known chromosomes containing the DM2 $(CCTG)_n$ expansion and 160 phase-known normal chromosomes.

Determination of LD

To determine LD between markers near the DM2 $(CCTG)_n$ repeat and chromosome disease status, we used χ^2 contingency-table tests for each marker. A multipoint haplotype method employed by Borrego et al. (2003) and Cheng et al. (2003) was used, in which subhaplotypes of all possible widths were examined for association with disease. For each marker, the smallest nominal *P* value of the χ^2 statistic was recorded for all haplotype windows containing the marker. For these analyses, reconstructed haplotypes were used, and only the 103 normal haplotypes with no missing alleles were included. Initial sensitivity analyses indicated that the multipoint results depended greatly on microsatellite marker 814L21-GT1. Therefore, analyses were also performed with that marker excluded. Permutation tests were performed by randomly labeling sets of 17 haplotypes as "diseased" and the remainder as "normal" and then recomputing the overall test statistic. Empirical *P* values for the entire set of markers were thus obtained as the proportion of 1,000 permutation samples for which the permuted test statistic was more extreme than the observed statistic. Simple moment-based estimates of core ancestral haplotype frequencies and mutation age can be obtained as described by Borrego et al. (2003). In brief, a putative core ancestral haplotype was identified and treated as a single allele with frequencies p_{disease} among disease chromosomes and p_{normal} among normal chromosomes. The quantity $p_{\text{excess}} = (p_{\text{disease}} - p_{\text{normal}})/(1 - p_{\text{normal}})$ simultaneously highlights the area of greatest LD and, at its peak, serves as a crude estimate of the proportion of disease chromosomes descended from the major mutation (de la Chapelle and Wright 1998). A simple regression of $\log(p_{\text{excess}})$ on the genetic distance from the DM2 expansion (Borrego et al. 2003) can be used to estimate the age of the mutation, although it is difficult to assign confidence intervals when such moment-based approaches are used (Slatkin and Rannala 2000). For the regional recombination rate per megabase, we used the deCODE map (Kong et al. 2002). To supplement the haplotype analyses and obtain interval estimates for the mutation age, the program DMLE+ (Reeve and Rannala 2002), employing Bayesian multipoint population genetic modeling, was used to examine the data for evidence of a founding locus, using the entire set of 160 normal haplotypes.

Results

Linkage to 3q21 and Confirmation of DM2 $(CCTG)_n$ Expansion

Genomewide scans for linkage were performed on four kindreds (FIN01, I01, US01, and US02) with sets of 400 markers at 10-cM intervals. The highest individual and cumulative LOD scores were seen for markers in 3q21, when weakness, myotonia, and cataracts were considered together. No other markers yielded LOD scores exceeding those for 3q21. Thus, these kindreds were considered to show linkage to 3q21, the same region to which DM2 had been mapped (Ranum et al. 1998).

Subsequently, 13 additional kindreds meeting our clinical criteria (Moxley et al. 1998) were identified. Linkage analysis for all 17 families, through use of the markers shown in figure 1*A*, provided a peak multipoint LOD score of 19.521 at D3S3584. Using informative crossovers, we further narrowed the critical region to a 2.06-cM interval between D3S3584 and *RHO* (fig. 1*A*). Evidence of allele and haplotype sharing was seen, in three Finnish families, with markers D3S3584, 153F10-GT1, D3S3606, D3S3607, and 571C11-AG1. When markers derived from the BAC sequences were included, the peak multipoint LOD score was 23.445 and haplotype sharing extended to 436B3-AG1.

When checked for the DM2 $(CCTG)_n$ expansion in *ZNF9* (Liquori et al. 2001), all affected individuals showed a single allele by PCR analysis. Affected children presented with an apparent non-Mendelian inheritance, indicating that PCR amplified only the allele inherited from the unaffected parent. Segregation of the DM2 $(CCTG)_n$ mutant expansion in our kindreds was confirmed by Southern blot analysis. Using FIGE, we identified expansions ranging from approximately +4 kb to +27 kb, with a mean expansion size of ~17–18 kb. Figure 2*A* and *B* show the detection of the DM2 expansion by FIGE Southern blot analysis and a representative PROMM pedigree. Since Southern blot analysis can fail to detect expansions (individual II:6; fig. 2*B*), because of the unusual size and somatic heterogeneity of the $(CCTG)_n$ expansion, we also developed an RP-PCR assay to determine the presence of the mutation. Combining PCR analysis across the DM2 repeat with our FIGE Southern blot and/or RP-PCR analyses, we were able to unequivocally determine the presence of a DM2 $(CCTG)_n$ expansion in all affected individuals and to determine the size of the expansion in most of them.

Sequence analysis of normal alleles of the DM2-associated $(CCTG)_n$ repeat showed the same complex repeat motif (TG)20-24(TCTG)6-10(CCTG)11-16 as reported by Liquori et al. (2001). The majority of expansion carriers showed broad smears or multiple bands

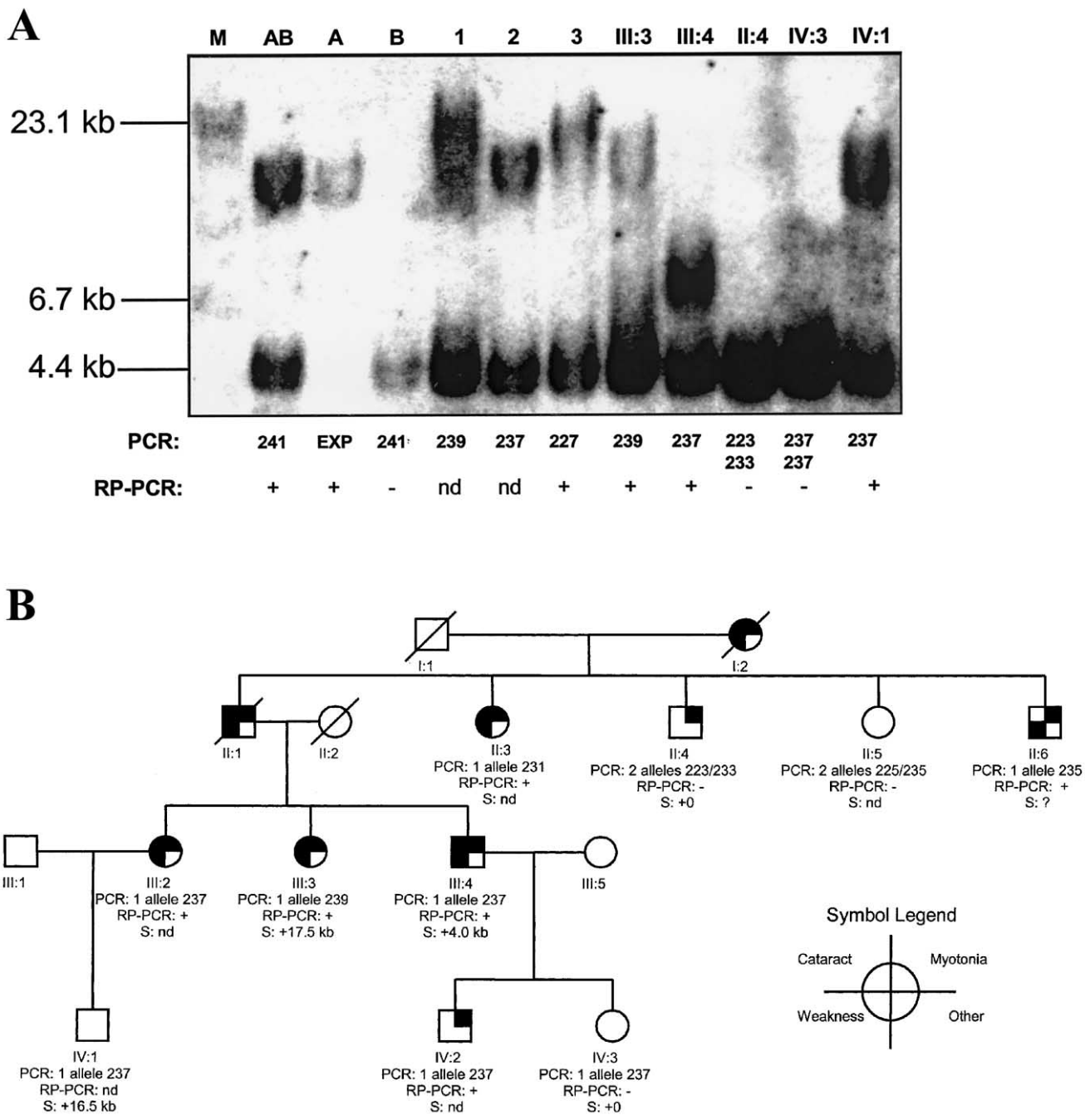

Figure 2 Molecular diagnosis of the DM2 $(CCTG)_n$ expansion mutation in an Italian family (I01) with PROMM and other selected cases. *A*, FIGE Southern blot showing expanded $(CCTG)_n$ alleles at the *DM2* locus. Shown beneath each lane are the PCR allele sizes across the DM2 repeat and the results (+/−) of the RP-PCR assay. Pedigree numbers in the lane headers refer to those shown in the pedigree (*B*). A and B are haploid hybrids for the normal and mutant chromosome 3, respectively; AB is the donor patient from which the hybrid cell lines were established; M is the size marker lane; and cases 1–3 are individual, unrelated patients. *B*, Pedigree of PROMM kindred I01 (Meola et al. 1996), illustrating commonly encountered diagnostic problems and the importance of using multiple molecular diagnostic tests. Individual II:4 exemplifies a false-positive diagnosis. He had myotonia but had two normal alleles and showed no expansion by either RP-PCR or Southern analysis ("S"). For individual II:6, who has myotonia and muscle weakness, Southern analysis gave an unclear molecular diagnosis, whereas RP-PCR clearly identified him as a mutation carrier. Individual IV:1 has a false-negative diagnosis. Although phenotypically normal, he has an expansion of +16.5 kb. Individual IV:3 is a true homozygote. Both RP-PCR and Southern analysis confirm the absence of the expansion, in spite of the presence of only a single allele.

by Southern blot analysis, indicating somatic instability. Thus, the expansion detected in our kindreds presenting with a highly variable clinical phenotype that was originally considered distinct from DM2 (Moxley et al. 1998) was the same type of expansion seen in DM2 (Liquori et al. 2001).

Verification of the Physical Map by STS-Content Mapping and FISH

To study the evolution of the DM2 $(CCTG)_n$ mutation, we constructed a comprehensive physical map of the DM2 region. All markers used were confirmed to be present on 814L21 by STS-content mapping. We also performed FISH analysis of this clone and verified that it contained only DNA localizing to 3q21. Chromosomal location of the genomic clones 814L21, 436B3, and 529F4 was confirmed by FISH. All three clones mapped to chromosome 3q21 (fig. 3*A* and 3*B*).

After confirming the location and excluding chimerism, the clones were hybridized in different combinations to extended DNA fibers to establish their mutual order and the distance separating 814L21 and 436B3. Double-color fiber-FISH experiments confirmed the order of the clones (figs. 1*B* and 3*C*). The average gap size between 814L21 and 436B3 was determined to be 227 kb (SD 59; $n = 9$).

Microsatellite Allele Sharing in Patients

With microsatellites closer to the DM2 expansion (221E20-AG1, 814l21-GT1, and 436B3-AG1), more extensive allele sharing was seen in the same three Finnish families as before. A subregion of this haplotype centromeric to the expansion was shared by three German, one U.S., one French, and one U.K. family (northern haplotype). In five families (one Spanish, one French, and three Italian) a different set of alleles was shared at 221E20-AG1 and 814L21-GT1 (southern haplotype) (fig. 4).

Microsatellites >350 kb from the repeat had allele frequencies on DM2 chromosomes that were similar to

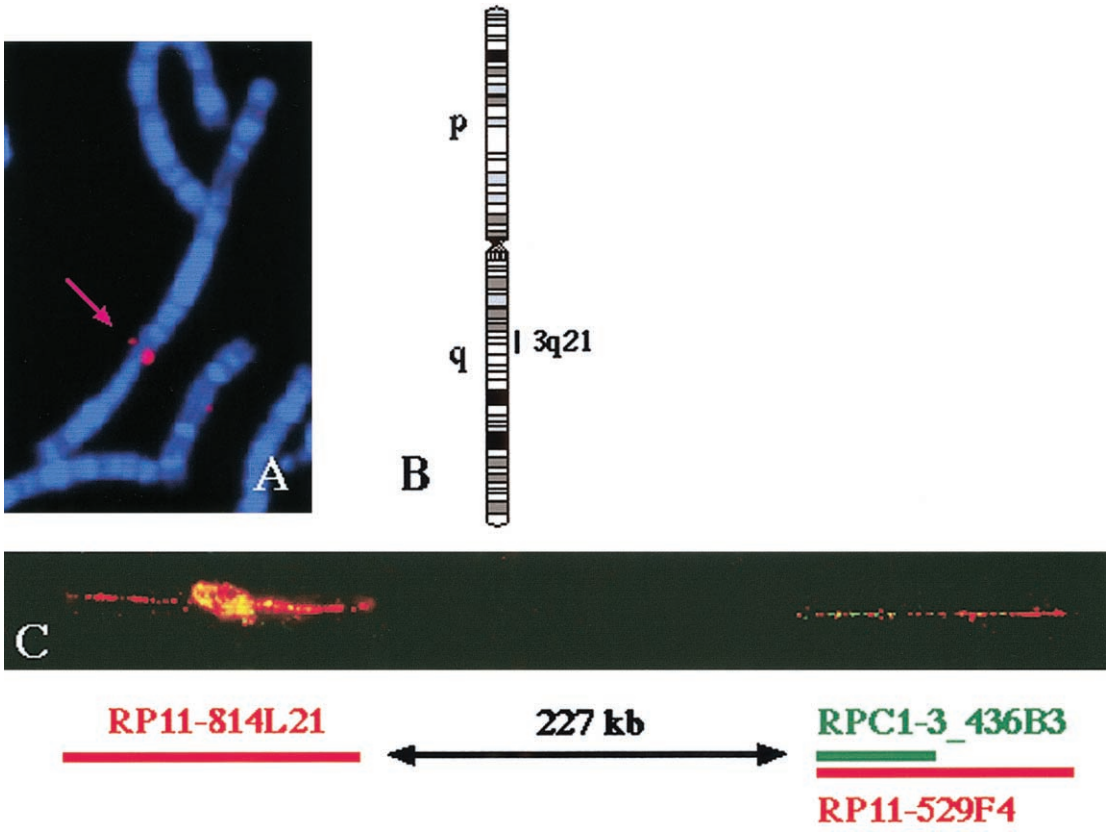

Figure 3 Chromosomal location and physical map of the BAC and PAC clones from the *ZNF9* region determined by FISH. *A,* RPC1-3_436B3 was assigned to 3q21 by metaphase FISH (*red*). *B,* Ideogram of human chromosome 3. *C,* Mutual order of RP11-814L21, RPC1-3 436B3, and RP11-529F4, and the size of the gap in the physical map determined by fiber-FISH. Cohybridization of the three clones shows the order RP11-814L21–RPC1-3_436B3–RP11-529F4. A schematic representation of the genomic clones is shown below the image. The approximate size of the gap between RP11-814L21 and RPC1-3 426B3 was estimated at 227 kb (SD 59 kb).

Marker	D01	CH01	I04	E02	I03	F002	I01	NY01	UK02	F01	D02	D03	D06	NY02	FIN01	FIN02	FIN04	Mb
D3S1589	166	147	164	nd	nd	nd	158	164	nd	160	170	168	168	162	158	168	164	- 3.042
D3S3584	150	152	150	nd	150	152	nd	149	152	152	152	160	150	152	154	154	154	- 1.756
D3S3606	173	177	169	nd	169	177	nd	173	183	185	185	163	171	169	171	171	171	- 1.750
D3S3607	nd	165	165	nd	169	165	nd	157	163	163	nd	167	nd	159	169	169	169	- 1.652
571C11_AG1	225	225	225	nd	223	210	nd	221	227	227	228	nd	228	nd	223	223	223	- 0.978
221E20-GT1	185	181	197	176	176	176	181	189	187	191	183	183	183	183	183	183	183	- 0.362
814L21-GT1	146	146	148	148	148	148	148	152	154	154	154	154	154	154	154	154	154	- 0.124
DM2	EXP	EXP	EXP	EXP	EXP	EXP	EXP	EXP	EXP	EXP	EXP	EXP	EXP	EXP	EXP	EXP	EXP	0.000
814L21-GT2	123	123	123	123	123	123	123	123	123	123	123	123	123	123	123	123	123	+ 0.013
436B3-AG1	254	254	254	254	250	257	257	260	252	257	257	258	257	254	254	257	257	+ 0.213
RHO	129	127	125	nd	125	129	nd	127	127	125/129	nd	129	nd	nd	125	nd	129	+ 0.361
D3S1587	227	227	227	nd	229	227	nd	229	229	229	nd	227	nd	nd	229	nd	229	+ 1.998

Northern Alleles

Southern Alleles

Figure 4 Shared microsatellite marker haplotypes in families with DM2 over 5 Mb flanking the DM2 mutation. The country of origin of samples is indicated (CH = Switzerland; D = Germany; E = Spain; F = France; FIN = Finland; I = Italy; NY = United States; UK = United Kingdom). The 154-bp allele at 814L21-GT1 and 183-bp allele at 221E20-GT1 are seen predominantly on DM2 chromosomes of northern European origin (Finland, Germany, United Kingdom, and France). The 148-bp and 176-bp alleles at these respective loci are seen predominantly on DM2 chromosomes of southern European origin (Spain, Italy, and France). Alleles in common are indicated by shading.

those seen in normal individuals. Markers 814L21-GT1 (located ~130 kb centromeric from the expansion) and 436B3-AG1 (located ~200 kb telomeric from the expansion) showed a preponderance of just two alleles on disease chromosomes, suggestive of disequilibrium with the repeat expansion. Normal chromosomes had nine alleles at 814L21-GT1. The 154-bp allele (population frequency 9%) was seen on 9 of the 17 DM2 chromosomes (53%). The 257-bp allele at marker 436B3-AG1 seen on 6 of the 17 expansion chromosomes (35%) was observed on only 1 of 153 normal chromosomes (<1%).

High-Resolution SNP Mapping of DM2 Chromosomes

Figure 5 shows the results of our high-resolution marker analysis of the DM2 region. Of the 22 SNPs interrogated, only 6 showed variation in the testing sample set and only 2 of these had a minor allele frequency >5%. All markers used in this study were determined to be in Hardy-Weinberg equilibrium. SNPs rs2341295 and TSC0176095 are located 171 bases apart on the same amplified fragment and were treated as a multiallele locus. Observed allele frequencies are shown in table E (online only).

Because of low polymorphism, there was no difference in allele frequencies between DM2 and normal chromosomes for five of the six SNPs. However, TSC873597, ~13–30 kb telomeric to the expansion, showed only the "C" allele on the 17 DM2 chromosomes. The frequency of "C" for normal chromosomes was 50%. A Fisher's exact test for this difference was highly significant ($P = 3.0 \times 10^{-5}$). In an unrelated group of 11 DM2 index cases, no instances of the AA genotype were seen, consistent with the presence of the "C" allele on the DM2 haplotype. Taken together, these data are consistent with a single origin for the DM2 mutation occurring on a chromosome bearing the "C" allele at TSC873597.

Characterization of Haplotypes in DM2 and Control Families

All 17 independent DM2 chromosomes were invariant for all markers from rs762570 to TSC873597, ~132–163 kb (the boxed region in fig. 5), and shared a single haplotype identical to the most common normal haplotype (fig. 6*A*). We observed a total of 10 different haplotypes on 160 independent normal chromosomes. The most common haplotype (A) was present on 46.8%. The second most common haplotype (B) was present on 41.25% and differed from A only at TSC873597 (fig. 6*A*). The 10 observed haplotypes and their evolutionary relationships to each other are shown in figure 6*B*. This is reminiscent of the situation in DM1 (Imbert et al. 1993; Neville et al. 1994). Taken together, these data suggest a single founding mutation in patients with DM2 from diverse European populations.

LD in the DM2 Region

The permutation tests to determine LD in the DM2 region were highly significant (*P* values <.001) whether or not marker 814L21-GT1 was included (fig. 7). With 814L21-GT1 included, the evidence peaks ~120 kb centromeric to the DM2 expansion. When 814L21-GT1

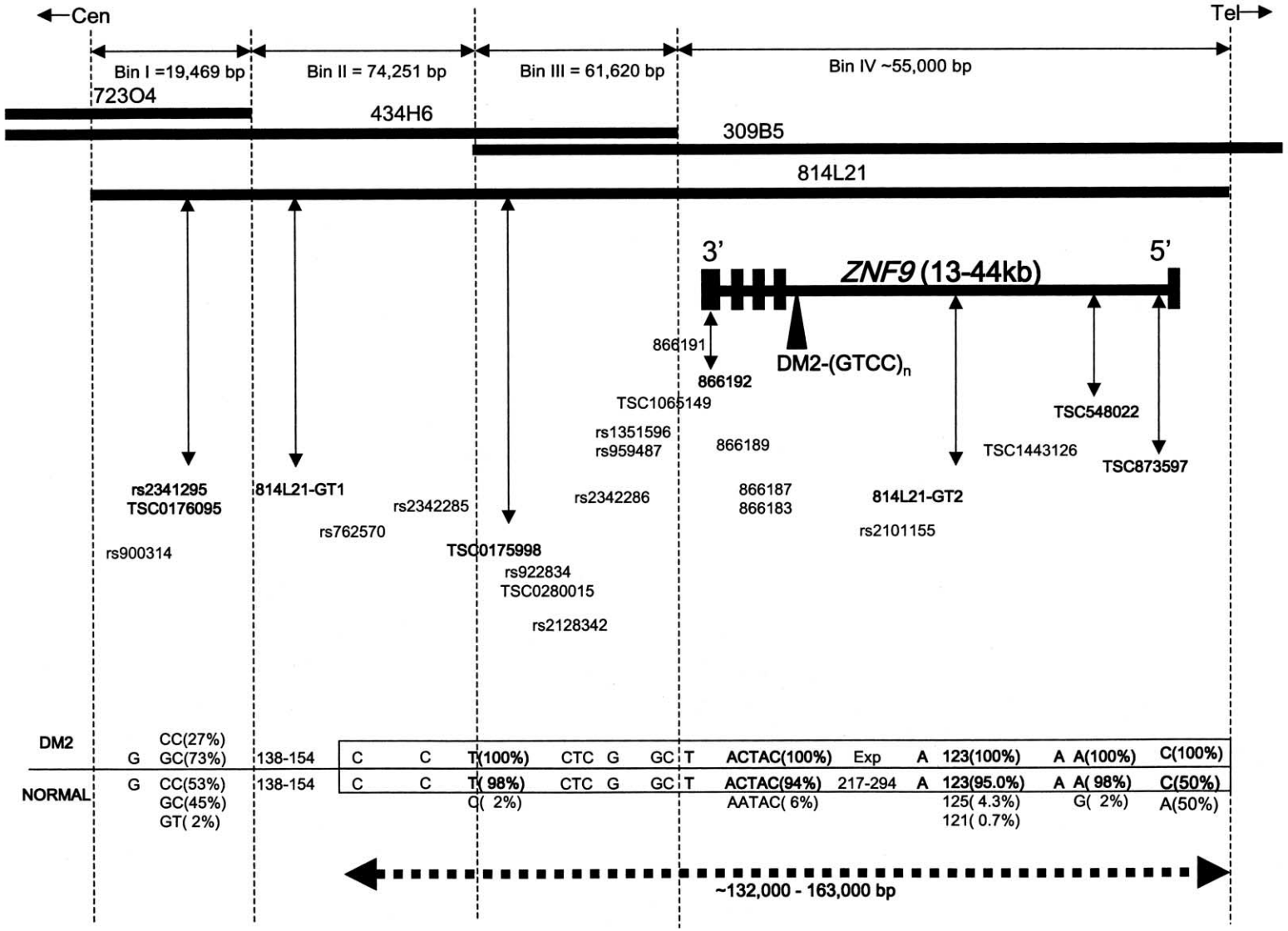

Figure 5 Physical map of the *ZNF9* region in 3q21 with the DM2 $(CCTG)_n$ expansion mutation (not drawn to scale). Bins are determined by overlap with the three other BAC clones available. Alleles found on DM2 and normal chromosomes are indicated, along with their frequencies. Approximately 30 kb of unordered fragments could be located either in intron 1 of *ZNF9* or telomeric. Thus, the genomic size of *ZNF9* can be estimated as at least 13 kb but could be as large as 44 kb. Consequently, the invariant haplotypes on DM2 chromosomes (*boxed region*) could be as small as 132 kb or as large as 163 kb.

A

Haplotype	rs762570	rs2342285	TSC175998	rs922834	TSC0280015	rs2128342	rs2342286	rs959487	rs1351596	TSC1065149	886191	886192	886189	886183	886187	DM2	rs2101155	814L21-GT2	TSC1443126	TSC548022	TSC873597	Obs/N
DM2	C	C	T	G	C	G	G	T	C	T	A	C	T	A	C	EXPANDED	A	123	A	A	C	17/17
A	C	C	T	G	C	G	G	T	C	T	A	C	T	A	C	193-229	A	123	A	A	C	75/160
B	C	C	T	G	C	G	G	T	C	T	A	C	T	A	C	193-231	A	123	A	A	A	68/160
C	C	C	T	G	C	G	G	T	C	T	A	A	T	A	C	203, 205, 211, 213	A	123	A	A	A	5/160
D	C	C	T	G	C	G	G	T	C	T	A	C	T	A	C	197, 199, 209	A	125	A	A	C	3/160
E	C	C	T	G	C	G	G	T	C	T	A	C	T	A	C	221, 223	A	123	A	G	C	3/160
F	C	C	T	G	C	G	G	T	C	T	A	C	T	A	C	207, 211	A	125	A	A	A	2/160
G	C	C	T	G	C	G	G	T	C	T	A	A	T	A	C	199	A	123	A	A	C	1/160
H	C	C	T	G	C	G	G	T	C	T	A	A	T	A	C	199	A	125	A	A	C	1/160
I	C	C	T	G	C	G	G	T	C	T	A	C	T	A	C	213	A	121	A	A	A	1/160
J	C	C	C	G	C	G	G	T	C	T	A	C	T	A	C	211	A	123	A	A	C	1/160

B

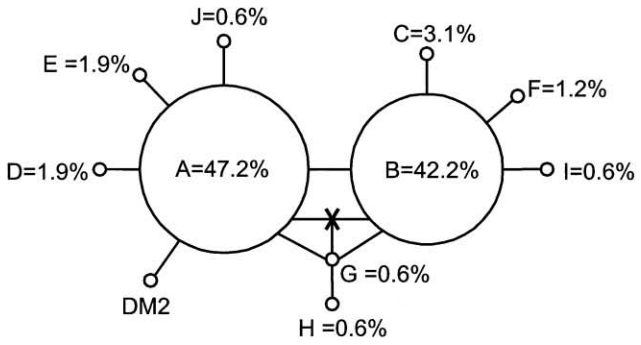

Figure 6 *A*, Haplotypes observed across the DM2 region. Ten normal haplotypes (A–J) are shown, along with the DM2 haplotype, which is identical to haplotype A except for the presence of the DM2 $(CCTG)_n$ expansion. *B*, Haplotype evolutionary network based on parsimony. The areas of circles representing each haplotype are roughly proportional to the frequency of the haplotype being represented. Each haplotype is one mutational step from all of the haplotypes to which it is connected by a line. Haplotypes G and H are the only two haplotypes for which relationships are unclear. Haplotype G is either the result of a recombination or gene conversion event between the common haplotypes A and B (indicated by X) or the result of a repeat mutation (homoplasy), in which haplotype A changed by acquiring the mutation that is diagnostic for B or vice versa.

was removed from the analysis, a core haplotype from rs900314 to TSC873597 (fig. 5) was apparent on 11/17 DM2 haplotypes but on only 10/103 normal haplotypes ($P = 2.2 \times 10^{-6}$, Fisher's exact test). Alleles 148 and 154 of 814L21-GT1 occur almost exclusively in disease haplotypes and occur in 10/11 of the disease chromosomes with the putative extended core haplotype. These observations appear consistent with a microsatellite mutation occurring on the core haplotype sometime later than the original mutation event. This scenario is further supported by the fact that affected kindreds with allele 148 versus allele 154 appear to roughly correspond to families of southern European versus northern European ancestry. When 814L21-GT1 is removed from the analysis, the evidence for LD is constant across a broad interval (fig. 7). Under this hypothesis, the bias in the higher curve (fig. 7) stems from the proposed microsatellite mutation, combined with the greater informativeness of the 814L21-GT1 microsatellite marker compared with the surrounding SNP markers.

When 814L21-GT1 was excluded, the simple moment-based procedure gave an estimate of 208 generations since the founding haplotype, accounting for a

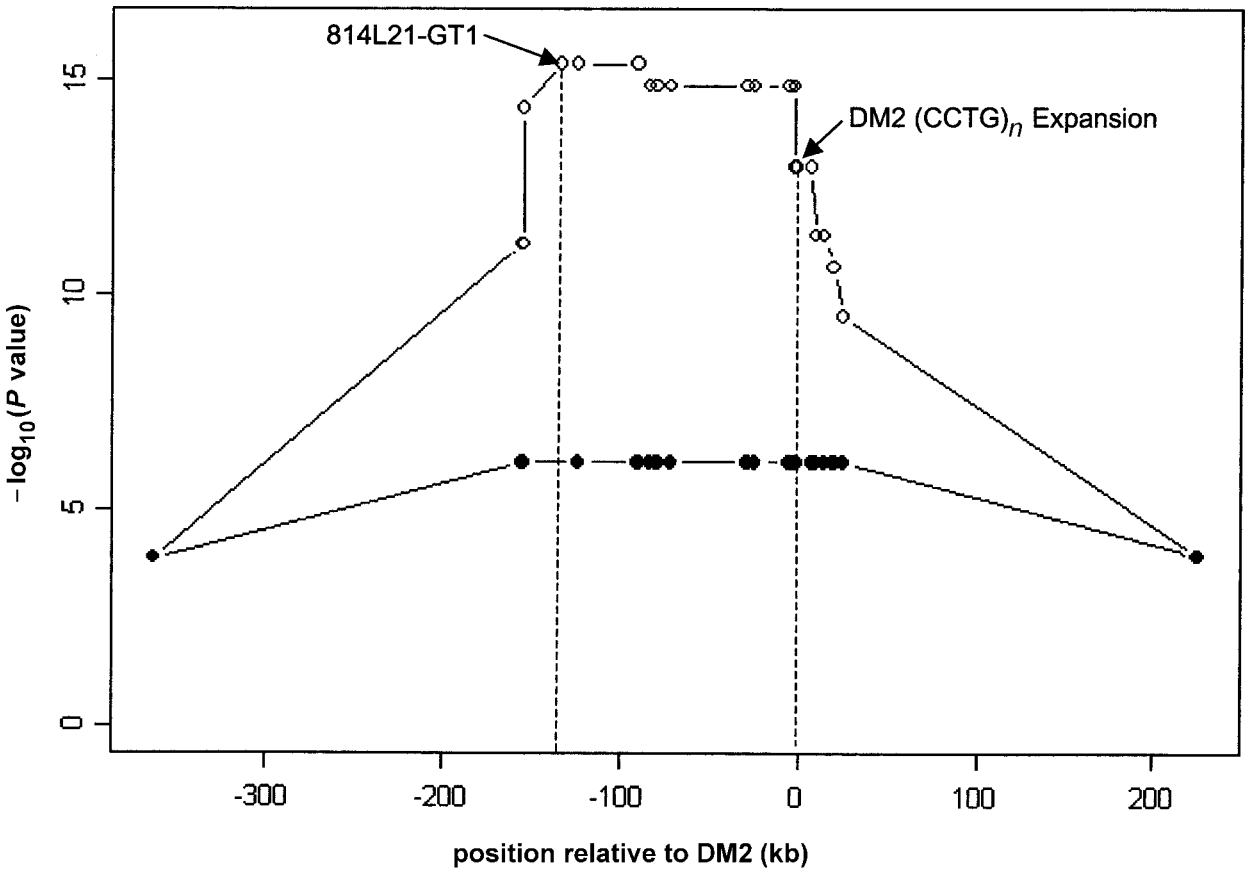

Figure 7 Evidence for LD with disease status for markers near the DM2 $(CCTG)_n$ expansion. The *Y*-axis shows nominal *P* values (on a $-\log_{10}$ scale) for the moving-window haplotype contingency-table test. The evidence when marker 814L21-GT1 is included (*unblackened circles*) peaks centromeric to the expansion and is much stronger than when the marker is excluded (*blackened circles*). Permutation-based *P* values for the entire set of markers gave $P < .001$ for both curves.

p_{excess} of 60.9% of the disease haplotypes. The estimated mutation age depended somewhat on the assumed historical population growth rate, with 90% credible intervals of 380–465 generations, for a growth rate of 5% per generation, and 515–540 generations, for a growth rate 2% per generation. Although these estimates are higher than that provided by the moment-based approach, they are dependent on population modeling assumptions. Using an average generation time of 20 years, the estimates correspond to a mutation age range of ~4,000–11,000 years. We view the data, when taken together, as consistent with the DM2 mutation originating in Europe but being ancient enough to be present in several European subpopulations.

Discussion

We studied 17 kindreds with disease that was originally classified as PDM or PROMM on the basis of clinical presentation and was therefore considered a distinct clinical entity from DM2 (Moxley et al. 1998). Here, we show linkage to the DM2 region in 3q21 (Ranum et al. 1998) and confirm the presence of the DM2 $(CCTG)_n$ expansion mutation (Liquori et al. 2001; Day et al. 2003) in all of our patients. It has been suggested that PROMM/DM2 is predominantly a disease of German or northern European origin (Day et al. 2003). Our study of patients from diverse (southern and northern) European populations indicates that PROMM/DM2 is not limited to patients of northern European descent but is more widely spread throughout European populations.

Since the molecular diagnosis and accurate sizing of the DM2 expansion mutation can be difficult and unreliable because of the unprecedented size of the expansion (Liquori et al. 2001), we developed a FIGE-based protocol (fig. 2*A*) and an RP-PCR assay. Approximately 5%–10% of normal individuals have two identically sized alleles for the polymorphic DM2 repeat; thus, PCR across the repeat is a useful first test for DM2. With our RP-PCR assay, homozygous normal individuals can be

readily distinguished from mutation carriers with an expanded allele resistant to standard PCR. The RP-PCR procedure is also useful for confirmation when Southern blot analysis is equivocal (~20% of the time [Day et al. 2003]). Our FIGE-based Southern blot approach provides a means for reliable size determination of the repeat beyond the resolution of standard gel electrophoresis (>20 kb). Using these methods in combination, we were able to unequivocally identify all mutation carriers in our sample set.

Initial analysis of shared microsatellite haplotypes in our 17 European kindreds identified a southern and a northern European haplotype and suggested the possibility of population-specific or regional founder effects (fig. 4). To further study the evolution of the DM2 repeat, we generated a high-resolution genetic and physical map of the DM2 region (figs. 1 and 5). Further fine mapping of disease chromosomes with the additional microsatellite and SNP markers showed complete conservation of a single common haplotype shared among all affected individuals from the 17 kindreds studied (figs. 5 and 6*A*). Comparison with population-matched unaffected individuals showed that the DM2 expansion segregates on the most common normal haplotype (A), with the expansion being the only difference (fig. 6*A*). Interestingly, in the 200-kb region flanking the DM2 repeat, there are relatively few microsatellite markers, and the available SNPs were not very polymorphic, suggesting that this region is part of an invariant haplotype block. This notion is further supported by the identification of only two major haplotypes (A and B), which together account for ~89% of all observed haplotypes.

On the basis of the highly statistically significant LD (fig. 7) and the extent of LD observed (~132–163 kb; figs. 5 and 7), we estimated the age of the DM2 mutation at ~4,000–11,000 years. These data, taken together with the lack of reports for DM2 in non-European populations, suggest a single (or a few) founding mutation(s) for the DM2 expansion in patients of European descent after the migration out of Africa. Thus, the situation in DM2 is similar to that seen in DM1, in which all patients of European descent segregate the $(CTG)_n$ expansion on a single haplotype (A). However, the fact that the LD seen in DM1 is significantly smaller (~40 kb [Imbert et al. 1993; Neville et al. 1994]) and the fact that DM1 is found in the Japanese population (Yamagata et al. 1998) suggest that the DM2 expansion mutation occurred more recently. The large variability in estimated ages is not unique to the present data set (see, for example, Slatkin and Rannala 2000), but the evidence supports the conclusion that the mutation, although not extremely ancient, may be old enough to be widespread in European populations.

The observed LD extends for a 3–4 times greater distance on the centromeric side of the DM2 repeat than the telomeric side (fig. 7), whether or not the microsatellite marker 814L21-GT1 is included in the calculations. The apparent skewing of the LD region could result from sampling variability or from a lower recombination rate to the centromeric side. Alternatively, the LD peak at 814L21-GT1 (when the marker is included) might reflect an unknown *cis*-acting element contributing to the DM2 expansion, as has been suggested for DM1 and other trinucleotide-repeat diseases (Brock et al. 1999). Additional evidence for the involvement of flanking sequences comes from the variable stability of similar $(CAG)_n$ repeats at different disease loci (Richards et al. 1996; Brock et al. 1999; Cleary et al. 2002) and from transgenic mouse models of trinucleotide-repeat instability (Gourdon et al. 1997; Monckton et al. 1997). Although the nature of such a *cis* element(s) is currently unknown, recent in vitro studies suggest that the distance of the repeat to the replication origin may be an important factor (Cleary et al. 2002).

In conclusion, patients of non–northern European descent presenting with progressive myotonic myopathy should be examined for the DM2 $(CCTG)_n$ expansion mutation in 3q21, if negative for the DM1 $(CTG)_n$ expansion mutation. The identification of the same genetic mutation in patients presenting with highly varied clinical phenotypes with predominantly or exclusively proximal muscle involvement (PDM and PROMM), in contrast to the distal (and proximal) muscle involvement described in kindreds with DM2 (Day et al. 1999; Ranum et al. 1998), indicates that the clinical manifestations caused by the $(CCTG)_n$ expansion mutation are more varied than initially appreciated (Moxley et al. 1998) and suggests that modifying genetic factors and genetic background act in concert with the $(CCTG)_n$ expansion mutation.

Acknowledgments

We are grateful to the participating families for their cooperation. R.K. would like to thank N. Z. Moore and T. Ahmed, for assistance, and S. Colella, for advice on pyrosequencing, as well as D. Lee, S. McWhinney, M. Holloway, X. Gao, and D. Wang, for assistance, and the Human Cancer Genetics Program Genotyping-Sequencing Unit (Ohio State University), for technical assistance with genotyping in the early stages of this study. Samples from two German families with PROMM/DM2 (D01 and D02) were also studied by L. P. W. Ranum and colleagues in a separate study. We thank the Association Française contre les Myopathies for their support with the procurement of French patient samples. We wish to thank the European Neuro-Muscular Centre for their continued support of the International Working Group on DM2/PROMM and Other Myotonic Dystrophies. This study was supported by grants from the Juselius Foundation, Ohio State University, Muscular Dystrophy Association U.S.A., the National Institutes of Health (grant R01 AR48171 and, in part,

grant P30 CA16058, both to R.K.), Medicinska understödsföreningen Liv och Hälsa r.f. (to B.U.), the Folkhälsan Institute of Genetics (to R.K. and B.U.), MURST-Italy (to G.M.), the Research and Science Foundation of Farmos, and the Research Foundation of the University of Helsinki (to R.S.).

Electronic-Database Information

The URLs for data presented herein are as follows:

dbSNP Home Page, http://www.ncbi.nlm.nih.gov/SNP/
GenBank, http://www.ncbi.nlm.nih.gov/Genbank/ (for RP11-814L21 [accession number AC022944], RP11-309B5 [accession number AC135587], RP11-723O4 [accession number AC112484], and RP11-434H6 [accession number AC108673], and chromosome 3 contig [accession number NT_006025])
Gene Viewer, Cancer Genome Anatomy Project (CGAP), http://gai.nci.nih.gov/cgi-bin/GeneViewer.cgi (for CGAP SNPs)
NCBI Reference Sequence (RefSeq), http://www.ncbi.nlm.nih.gov/RefSeq/
Online Mendelian Inheritance in Man (OMIM), http://www.ncbi.nlm.nih.gov/Omim/ (for DM1, DM2, and PROMM)
SNP Consortium, The, http://snp.cshl.org/

References

Abbruzzese C, Krahe R, Liguori M, Tessarolo D, Siciliano MJ, Ashizawa T, Giacanelli M (1996) Myotonic dystrophy phenotype without expansion of (CTG)n repeat: an entity distinct from proximal myotonic myopathy (PROMM)? J Neurol 243:715–721

Ashizawa T, Epstein HF (1991) Ethnic distribution of myotonic dystrophy gene. Lancet 338:642–643

Bassez G, Attarian S, Laforet P, Azulay JP, Rouche A, Ferrer X, Urtizberea JA, Pellissier JF, Duboc D, Fardeau M, Pouget J, Eymard B (2001) Proximal myotonial myopathy (PROMM): clinical and histology study. Rev Neurol 157: 209–218

Borrego S, Wright FA, Fernandez RM, Williams N, Lopez-Alonso M, Davuluri R, Antinolo G, Eng C (2003) A founding locus within the RET proto-oncogene may account for a large proportion of apparently sporadic Hirschsprung disease and a subset of cases of sporadic medullary thyroid carcinoma. Am J Hum Genet 72:88–100

Brock GJ, Anderson NH, Monckton DG (1999) Cis-acting modifiers of expanded CAG/CTG triplet repeat expandability: associations with flanking GC content and proximity to CpG islands. Hum Mol Genet 8:1061–1067

Brook JD, McCurrach ME, Harley HG, Buckler AJ, Church D, Aburatani H, Hunter K, Stanton VP, Thirion JP, Hudson T, Sohn R, Zemelman B, Snell RS, Rundle SA, Crow S, Davies J, Shelbourne P, Buxton J, Jones C, Juvonen V, Johnson K, Harper PS, Shaw DJ, Housman DE (1992) Molecular basis of myotonic dystrophy: expansion of a trinucleotide (CTG) repeat at the 3′ end of a transcript encoding a protein kinase family member. Cell 68:799–808 (erratum 69:385)

Brownstein MJ, Carpten JD, Smith JR (1996) Modulation of non-templated nucleotide addition by Taq DNA polymerase: primer modifications that facilitate genotyping. Biotechniques 20:1004–1006, 1008–1010

Cheng R, Ma JZ, Wright FA, Lin S, Gao X, Wang D, Elston RC, Li MD (2003) Nonparametric disequilibrium mapping of functional sites using haplotypes of multiple tightly linked single-nucleotide polymorphism markers. Genetics 164: 1175–1187

Cleary JD, Nichol K, Wang YH, Pearson CE (2002) Evidence of cis-acting factors in replication-mediated trinucleotide repeat instability in primate cells. Nat Genet 31:37–46

Colella S, Shen L, Baggerly KA, Issa J-PJ, Krahe R (2003) Sensitive and quantitative universal Pyrosequencing methylation analysis of CpG sites. Biotechniques 35:146–152

Day JW, Ricker K, Jacobsen JF, Rasmussen LJ, Dick KA, Kress W, Schneider C, Koch MC, Beilman GJ, Harrison AR, Dalton JC, Ranum LP (2003) Myotonic dystrophy type 2: molecular, diagnostic and clinical spectrum. Neurology 60:657–664

Day JW, Roelofs R, Leroy B, Pech I, Benzow K, Ranum LP (1999) Clinical and genetic characteristics of a five-generation family with a novel form of myotonic dystrophy (DM2). Neuromuscul Disord 9:19–27

De la Chapelle A, Wright FA (1998) Linkage disequilibrium mapping in isolated populations: the example of Finland revisited. Proc Natl Acad Sci USA 95:12416–12423

Gourdon G, Radvanyi F, Lia AS, Duros C, Blanche M, Abitbol M, Junien C, Hofmann-Radvanyi H (1997) Moderate intergenerational and somatic instability of a 55-CTG repeat in transgenic mice. Nat Genet 15:190–192

Harper PS (2001) Myotonic dystrophy. W. B. Saunders, London

Heiskanen M, Karhu R, Hellsten E, Peltonen L, Kallioniemi OP, Palotie A (1994) High resolution mapping using fluorescence in situ hybridization to extended DNA fibers prepared from agarose-embedded cells. Biotechniques 17:928–929, 932–923

Imbert G, Kretz C, Johnson K, Mandel JL (1993) Origin of the expansion mutation in myotonic dystrophy. Nat Genet 4:72–76

International DM Consortium (IDMC) (2000) New nomenclature and DNA testing guidelines for myotonic dystrophy type 1 (DM1). Neurology 54:1218–1221

Irwin M, Cox N, Kong A (1994) Sequential imputation for multilocus linkage analysis. Proc Natl Acad Sci USA 91: 11684–11688

Kohler A, Burkhard P, Hefft S, Bottani A, Pizzolato GP, Magistris MR (2000) Proximal myotonic myopathy: clinical, electrophysiological and pathological findings in a family. Eur Neurol 43:50–53

Kong A, Gudbjartsson DF, Sainz J, Jonsdottir GM, Gudjonsson SA, Richardsson B, Sigurdardottir S, Barnard J, Hallbeck B, Masson G, Shlien A, Palsson ST, Frigge ML, Thorgeirsson TE, Gulcher JR, Stefansson K (2002) A high-resolution recombination map of the human genome. Nat Genet 31:241–247

Krahe R, Eckhart M, Ogunniyi AO, Osuntokun BO, Siciliano MJ, Ashizawa T (1995) De novo myotonic dystrophy mutation in a Nigerian kindred. Am J Hum Genet 56:1067–1074

Kress W, Mueller-Myhsok B, Ricker K, Schneider C, Koch MC,

Toyka KV, Mueller CR, Grimm T (2000) Proof of genetic heterogeneity in the proximal myotonic myopathy syndrome (PROMM) and its relationship to myotonic dystrophy type 2 (DM2). Neuromuscul Disord 10:478–480

Kruglyak L, Daly MJ, Reeve-Daly MP, Lander ES (1996) Parametric and nonparametric linkage analysis: a unified multipoint approach. Am J Hum Genet 58:1347–1363

Liquori CL, Ricker K, Moseley ML, Jacobsen JF, Kress W, Naylor SL, Day JW, Ranum LP (2001) Myotonic dystrophy type 2 caused by a CCTG expansion in intron 1 of ZNF9. Science 293:864–867

Mahadevan MS, Foitzik MA, Surh LC, Korneluk RG (1993) Characterization and polymerase chain reaction (PCR) detection of an *Alu* deletion polymorphism in total linkage disequilibrium with myotonic dystrophy. Genomics 15:446–448

Mankodi A, Thornton CA (2002) Myotonic syndromes. Curr Opin Neurol 15:545–552

Matsuura T, Ashizawa T (2002) Polymerase chain reaction amplification of expanded ATTCT repeat in spinocerebellar ataxia type 10. Ann Neurol 51:271–272

Meola G, Sansone V, Radice S, Skradski S, Ptacek L (1996) A family with an unusual myotonic and myopathic phenotype and no CTG expansion (proximal myotonic myopathy syndrome): a challenge for future molecular studies. Neuromuscul Disord 6:143–150

Monckton DG, Coolbaugh MI, Ashizawa KT, Siciliano MJ, Caskey CT (1997) Hypermutable myotonic dystrophy CTG repeats in transgenic mice. Nat Genet 15:193–196

Moxley RT 3rd, Meola G, Udd B, Ricker K (2002) Report of the 84th ENMC Workshop: PROMM (proximal myotonic myopathy) and other myotonic dystrophy-like syndromes: 2nd workshop. Neuromuscul Disord 12:306–317

Moxley RT 3rd, Udd B, Ricker K (1998) 54th ENMC International Workshop: PROMM (proximal myotonic myopathies) and other proximal myotonic syndromes. Neuromuscul Disord 8:508–518

Neville CE, Mahadevan MS, Barcelo JM, Korneluk RG (1994) High resolution genetic analysis suggests one ancestral predisposing haplotype for the origin of the myotonic dystrophy mutation. Hum Mol Genet 3:45–51

Newman B, Meola G, O'Donovan DG, Schapira AH, Kingston H (1999) Proximal myotonic myopathy (PROMM) presenting as myotonia during pregnancy. Neuromuscul Disord 9:144–149

Phillips MF, Rogers MT, Barnetson R, Braun C, Harley HG, Myring J, Stevens D, Wiles CM, Harper PS (1998) PROMM: the expanding phenotype. A family with proximal myopathy, myotonia and deafness. Neuromuscul Disord 8: 439–446

Ranum LP, Rasmussen PF, Benzow KA, Koob MD, Day JW (1998) Genetic mapping of a second myotonic dystrophy locus. Nat Genet 19:196–198

Reeve JP, Rannala B (2002) DMLE+: Bayesian linkage disequilibrium gene mapping. Bioinformatics 18:894–895

Richards RI, Crawford J, Narahara K, Mangelsdorf M, Friend K, Staples A, Denton M, Easteal S, Hori TA, Kondo I, Jenkins T, Goldman A, Panich V, Ferakova E, Sutherland GR (1996) Dynamic mutation loci: allele distributions in different populations. Ann Hum Genet 60:391–400

Ricker K, Grimm T, Koch MC, Schneider C, Kress W, Reimers CD, Schulte-Mattler W, Mueller-Myhsok B, Toyka KV, Mueller CR (1999) Linkage of proximal myotonic myopathy to chromosome 3q. Neurology 52:170–171

Ricker K, Koch MC, Lehmann-Horn F, Pongratz D, Otto M, Heine R, Moxley RT 3rd (1994) Proximal myotonic myopathy: a new dominant disorder with myotonia, muscle weakness, and cataracts. Neurology 44:1448–1452

Ricker K, Koch MC, Lehmann-Horn F, Pongratz D, Speich N, Reiners K, Schneider C, Moxley RT 3rd (1995) Proximal myotonic myopathy: clinical features of a multisystem disorder similar to myotonic dystrophy. Arch Neurol 52:25–31

Sallinen R, Latvanlehto A, Kvist AP, Rehn M, Eerola I, Chu ML, Bonaldo P, Saitta B, Bressan GM, Pihlajaniemi T, Vuorio E, Palotie A, Wessman M, Horelli-Kuitunen N (2001) Physical mapping of mouse collagen genes on chromosome 10 by high-resolution FISH. Mamm Genome 12:340–346

Schaffer AA (1996) Faster linkage analysis computations for pedigrees with loops for unused alleles. Hum Hered 46:226–235

Sermon K, Seneca S, De Rycke M, Goossens V, Van de Velde H, De Vos A, Platteau P, Lissens W, Van Steirteghem A, Liebaers I (2001) PGD in the lab for triplet repeat diseases—myotonic dystrophy, Huntington's disease and fragile-X syndrome. Mol Cell Endocrinol 183 Suppl 1:S77–S85

Slatkin M, Rannala B (2000) Estimating allele age. Annu Rev Genomics Hum Genet 1:225–249

Thornton CA, Griggs RC, Moxley RT 3rd (1994) Myotonic dystrophy with no trinucleotide repeat expansion. Ann Neurol 35:269–272

Udd B, Krahe R, CW-P, Falck B, Kalimo H (1997) Proximal myotonic dystrophy—a family with autosomal dominant muscular dystrophy, cataracts, hearing loss and hypogonadism: heterogeneity of proximal myotonic syndromes? Neuromusc Disord 7:217–228

Warner JP, Barron LH, Goudie D, Kelly K, Dow D, Fitzpatrick DR, Brock DJ (1996) A general method for the detection of large CAG repeat expansions by fluorescent PCR. J Med Genet 33:1022–1026

Wieser T, Bonsch D, Eger K, Schulte-Mattler W, Zierz S (2000) A family with PROMM not linked to the recently mapped PROMM locus DM2. Neuromuscul Disord 10:141–143

Yamagata H, Miki T, Nakagawa M, Johnson K, Deka R, Ogihara T (1996) Association of CTG repeats and the 1-kb Alu insertion/deletion polymorphism at the myotonin protein kinase gene in the Japanese population suggests a common Eurasian origin of the myotonic dystrophy mutation. Hum Genet 97:145–147

Yamagata H, Nakagawa M, Johnson K, Miki T (1998) Further evidence for a major ancient mutation underlying myotonic dystrophy from linkage disequilibrium studies in the Japanese population. J Hum Genet 43:246–249

Yan H, Papadopoulos N, Marra G, Perrera C, Jiricny J, Boland CR, Lynch HT, Chadwick RB, de la Chapelle A, Berg K, Eshleman JR, Yuan W, Markowitz S, Laken SJ, Lengauer C, Kinzler KW, Vogelstein B (2000) Conversion of diploidy to haploidy. Nature 403:723–724